Inclusive Scattering from Nuclei at $x > 1$ in the quasielastic and deeply inelastic regimes.

J. Arrington (Spokesperson), D.F. Geesaman, K. Hafidi, R. Holt,
D.H. Potterveld, P.E. Reimer, P. Solvignon
Argonne National Laboratory

D. Crabb, D.B. Day (Spokesperson), R. L. Lindgren, B. Norum
O. Rondon, K. Slifer, C. Smith, S. Tajima, K. Wang
University of Virginia

M. E. Christy, C. E. Keppel, L. Tang, V. Tvaskis
Hampton University

G. Niculescu, I. Niculescu
James Madison University

P.E. Bosted, R. Carlini, R. Ent, H. Fenker, D. Gaskell, T. Horn,
M.K. Jones, A.F. Lung, D.J. Mack, D.G. Meekins, J. Roche, G. Smith,
S. Wood, W. Vulcan, C. Yan
Thomas Jefferson National Accelerator Facility

B. Boillat, J. Jourdan, B. Krusche, G. Testa, R. Trojer
University of Basel

E.J. Beise, H. Breuer
University of Maryland

H. Mkrtchyan, V. Tadevosyan
Yerevan Physics Institute, Armenia

(Dated: July 7, 2006)

Inclusive scattering from nuclei at $x > 1$ is sensitive to the distribution of high momentum nucleons at low Q^2 values, and high momentum quarks at large Q^2 values. Large x data at 4 and 6 GeV are dominated by quasielastic and resonance production from high-momentum nucleons. With the 11 GeV beam, we propose to make measurements in the DIS region and provide clean measurements of the quark distributions in light and heavy nuclei for $x > 1$. The distribution of these superfast quarks (quarks carrying a momentum greater than that of a nucleon) is connected to the short distance structure of nuclei, and this is a promising region to examine for the importance of the underlying quark degrees of freedom in nuclear structure. In addition, data in the quasielastic region at very large x values, up to and exceeding $x = 3$, will extend previous studies of short range correlations in few-body and heavy nuclei.

Ratios of the structure functions at large x are are sensitive to both the distribution of high momentum nucleons and possible medium modification. The previous 4 and 6 GeV measurements and the extremely large x ($x \gtrsim 2$) QE measurements included here will constrain the high momentum nucleons and allow a study of the quark distributions in the kinematic region dominated by scattering from SRCs, which is expected to be very sensitive to modification to the nucleon structure. Note that both absolute quark distributions and EMC-style ratios for $x \gtrsim 1$ will be useful in understanding the EMC effect. While focussed on mapping out the distributions of superfast quarks and high momentum nucleons, these data also provide the large x data necessary to extract the QCD moments in nuclei at moderate to large Q^2 values.

I. INTRODUCTION

Previous measurements of inclusive scattering from nuclei have been made for a range of targets at SLAC[1, 2] and at 4 and 6 GeV at JLAB [3–5]. These data have been important sources of information on the momentum distribution of nucleons in nuclei, with an emphasis on high-momentum nucleons and y-scaling studies that are sensitive to the reaction mechanism and have allowed for tests of various theoretical models of inclusive scattering.

This proposal requests time to make inclusive electron scattering measurements with both few-body nuclei and heavy nuclei at high momentum transfers. Measurements at the largest x values are sensitive to high momentum nucleons in the nucleus (momenta in excess of 1000 MeV/c for the kinematics of this proposal), and provide clean information on the high momentum components of the spectral function. The measurements with few-body nuclei allow comparisons with essentially exact calculations of nuclear wave functions and provide an important complement to the coincidence $A(e, e'p)$ and $A(e, e'NN)$ measurements already completed or approved. The measurements with heavy nuclei should allow extrapolation to nuclear matter where again rigorous calculations can be performed and compared to the data. In addition to using the data to directly constrain the spectral function at very high momenta, we will use the nuclear dependence of the cross section to study the nature of the short–range correlations that are the main source of the high momentum nucleons. By comparing the distribution of high momentum nucleons in heavy nuclei to those measured in ^{2}H we can look for signatures of NN short range correlations. Measurements on ^{3}He and ^{4}He will provide significantly improved information on contributions from multi–nucleon short range correlations. Absolute cross section measurements in this kinematic region will be important in constraining final state interactions which can interfere with the interpretation of the cross section ratios in terms of short range correlations.

In addition to extending studies of high momentum nucleons and short range correlations in nuclei, this data will allow us to extract the nuclear structure functions at large x values. The quark distributions in nuclei at large x are poorly understood, and this will provide the first clean, high-precision measurement of the distribution of so-called "superfast" quarks. These quark distributions provide an additional way to look for the effect of short range correlations, but also provide high sensitivity to non-hadronic components of nuclear structure in these high density, short range configurations within nuclei.

Finally, these data will allow us to extend measurements of duality and scaling in nuclei, which are related to the connection between the quark and hadronic pictures of nuclear structure, and will provide the data necessary to make precision measurements of QCD moments in nuclei.

II. TECHNICAL PARTICIPATION OF RESEARCH GROUPS

This lead institutions for this proposal are Argonne National Lab and the University of Virginia. The Medium Energy Physics group at Argonne has responsibility for the initial optics design of the SHMS, field maps and verification of the optics of the SHMS. The University of Virginia nuclear physics group plans to design, build, and commission the atmospheric gas Čerenkov for the SHMS.

III. HIGH MOMENTUM COMPONENTS AND SHORT RANGE CORRELATIONS

High energy electron scattering from nuclei can provide important information on the wave function of nucleons in the nucleus. With simple assumptions about the reaction mechanism, scaling functions can be deduced that should scale (*i.e.* become independent of length scale or momentum transfer)

and which are directly related to the momentum distribution of nucleons in a nucleus. Several theoretical studies [6–9] have indicated that such measurements may provide direct access to short range nucleon-nucleon correlations.

The simple impulse approximation picture breaks down when the final-state interactions (FSI) of the struck nucleon with the rest of the nucleus are included. Previous calculations [10–18] suggest that the contributions from final state interactions should vanish at sufficiently high Q^2. Figure 1 shows the Q^2 dependence of the scaling function $F(y)$. The data show a clear approach to a scaling limit for both deuterium and heavy nuclei at large $-y$ values for $Q^2 > 3$ GeV^2, where y corresponds to the initial momentum of the struck nucleon along the direction of the virtual photon.

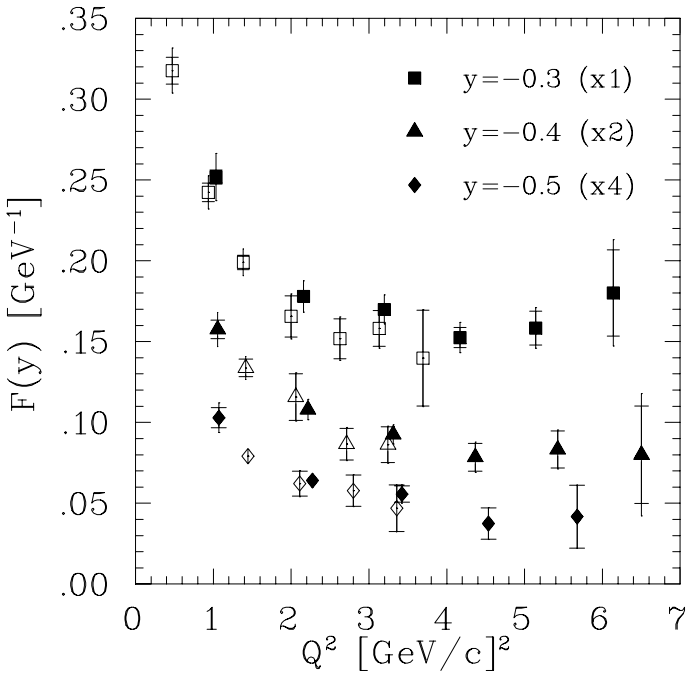

FIG. 1: Scaling function $F(y, Q^2)$ as a function of Q^2 for fixed y values. There is a clear onset of scaling for $Q^2 \approx 3$ GeV^2. Data are from [2] and [3].

While the observation of a y-scaling limit and the plateaus in the ratios of heavy nuclei to deuterium and ^{3}He is suggestive of an approach to the impulse approximation limit, it is not definitive. Even if scaling is observed, that does not insure that the scaling function is directly connected to the momentum distribution. Some calculations [8, 19] have pointed out that while the FSI of a struck nucleon with the mean field of the rest of the nucleus is a rapidly decreasing function of Q^2, the FSI of the struck nucleon with a correlated, high-momentum nucleon may show a very weak Q^2-dependence.

One approach to this issue has been to focus on cross section ratios in the region where the scattering is expected to be dominated by short range correlations [20]. In the large x region where correlations should dominate,

$$\begin{aligned}\sigma(x,Q^2) &= \sum_{j=1}^{A} A\frac{1}{j}a_j(A)\sigma_j(x,Q^2) \\ &= \frac{A}{2}a_2(A)\sigma_2(x,Q^2) + \frac{A}{3}a_3(A)\sigma_3(x,Q^2) + ...,\end{aligned}$$

where the constants $a_j(A)$ are proportional to the probability of finding a nucleon in a j-nucleon correlation, which should fall rapidly with j as nuclei are dilute. The cross section σ_j is the cross

section for scattering from a j-nucleon correlation, so $\sigma_2(x,Q^2) = \sigma_{eD}(a,Q^2)$ and $\sigma_j(x,Q^2) = 0$ for $x > j$. Even if there are Q^2-independent final state interactions coming from rescattering between nucleons in a short range correlation, this effect should be essentially identical for short range configurations in heavy and light nuclei. Thus, the final state interactions should cancel in the cross section ratio in the region dominated by SRCs, providing a test of SRC dominance, and a measure of the relative contribution from SRCs in different nuclei. So if the offshell effects and FSI largely cancel in the ratio as suggested by the Generalized Eikonal Approximation [21], one can take cross section ratios in kinematics where j-nucleon correlations dominate to extract the relative probability of finding a j-nucleon correlation in the two nuclei. Neglecting motion of the correlations in the nucleus, this implies:

$$\frac{2}{A}\frac{\sigma_A(x,Q^2)}{\sigma_D(x,Q^2)} = a_2(A)\Big|_{1<x\leq 2}$$
$$\frac{3}{A}\frac{\sigma_A(x,Q^2)}{\sigma_{A=3}(x,Q^2)} = a_3(A)\Big|_{2<x\leq 3}$$

Because of motion of the nucleons in the nucleus, a single nucleon will contribute some strength above $x = 1$, and a 2-nucleon correlation will have a small contribution for $x > 2$. Thus, one needs to avoid the region very close to $x = (j-1)$ when trying to isolate scattering from a j-nucleon correlation.

A combined analysis of several SLAC measurements at $x > 1$ showed that in the region where two-nucleon SRCs were expected to dominate, $1.5 \lesssim x < 2$, the ratio of the cross section of heavier nuclei to deuterium was independent of x in this region and showed little Q^2 dependence [22] as shown in Figure 2. This is consistent with the impulse approximation expectation if the scattering is dominated from short range correlations which are essentially identical in heavy nuclei and deuterium. Ref. [22] presented the extracted ratios to deuterium for ^{3}He, ^{4}He, ^{12}C, ^{27}Al, ^{56}Fe, and ^{197}Au for a Q^2 values up to 2–3 GeV^2, depending on the target.

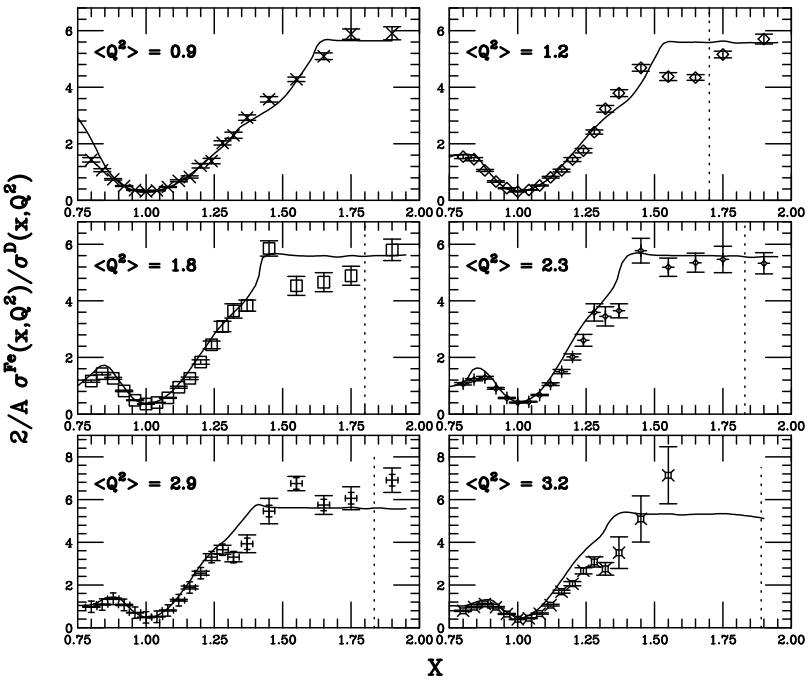

FIG. 2: Cross section (A/^{2}H) ratios at large x for Fe [22].

Measurements by the CLAS collaboration at Jefferson Lab [23] performed a similar analysis, taking ratios of ^{4}He, ^{12}C, and ^{56}Fe to ^{3}He (^{2}H data were not available at these kinematics) in the region of 2N SRC dominance. The ratios were consistent with the SLAC results, and expanded the Q^2 range, showing the effect of final state interactions at lower Q^2 values (down to 0.6 GeV^2), and providing measurements of the A/^{3}He ratios up to 2-2.5 GeV^2. The data from E89-008 [24] also examined these ratios, providing measurements of the A/^{2}H ratios at much larger Q^2 (Fig. 3, but with quite limited x coverage for the deuterium target, extending only a small range into the plateau region. Unfortunately, none of these extractions is ideal for a precise understanding of the contribution of SRCs. The SLAC result combined data from multiple experiments, which had to be interpolated to form the ratios at fixed Q^2. The CLAS results are obtained from a ratio to ^{3}He, combined with the ^{3}He/^{2}H ratios from SLAC, and is limited to relatively low Q^2. The Hall C data go to large Q^2 and provide absolute cross sections in addition to the ratios, but have very limited coverage at the largest x values.

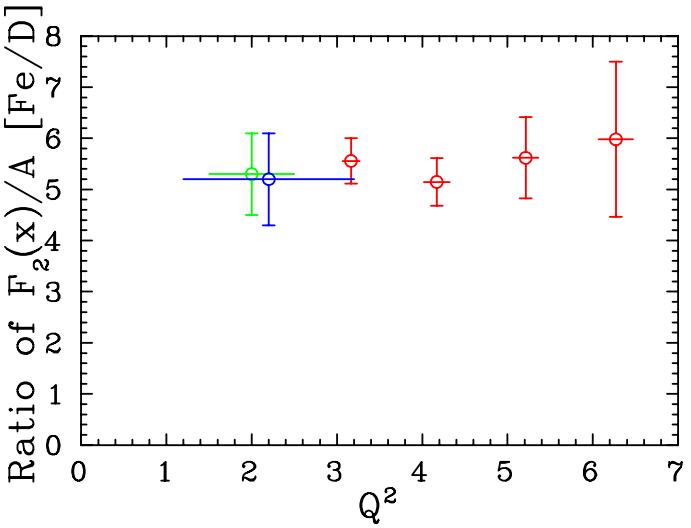

FIG. 3: Cross section (A/^{2}H) ratios at large x from SLAC (blue), and CLAS (green) measurements, averaged over the Q^2 range of the measurements, and the ratio from the Hall C measurements (red) shown as a function of Q^2.

This procedure was extended to the three-nucleon SRC region by a later CLAS measurement [25], which took an expanded data set and examined the A/^{3}He ratios up to $x \approx 3$. Figure 4 shows the ratios for this measurement, where one can observe that the ratios are x-independent in the regions of $1.5 < x < 2$ and $2.25 < x < 3$, consistent with the model of scattering from 2N and 3N SRCs. Data at large x was statistics limited, and the extracted ratios in the 3N SRC region are dominated by data with $1.4 < Q^2 < 1.6$ GeV^2, under the assumption that the onset of scaling for the 3N SRC region is consistent with the onset of scaling for 2N, where the data was sufficient to map out the Q^2 dependence in detail. Because of this, there is no direct test of the Q^2 independence of the ratio, and the extracted ^{56}Fe/^{3}He ratio changes by 20% as one varies the Q^2 range included, as shown in Fig. 18 of Ref. [26].

The measurements proposed here will have several advantages over the previous data. In the 2N SRC region, we will take ratios of heavier nuclei directly to deuterium, rather than taking ratios to ^{3}He as was done in CLAS, and then using the SLAC global analysis of ^{3}He and ^{2}H measurements to extract a_2. For ^{3}He, we will make measurements at larger Q^2 to test the Q^2 independence of the cross section ratio for $x > 2.25$, as well as providing higher statistics and measurements in a larger range of heavy nuclei. Finally, the previous measurements rely on cancellation of final state interactions between different nuclei in the plateau regions. One would expect only small differences in the final

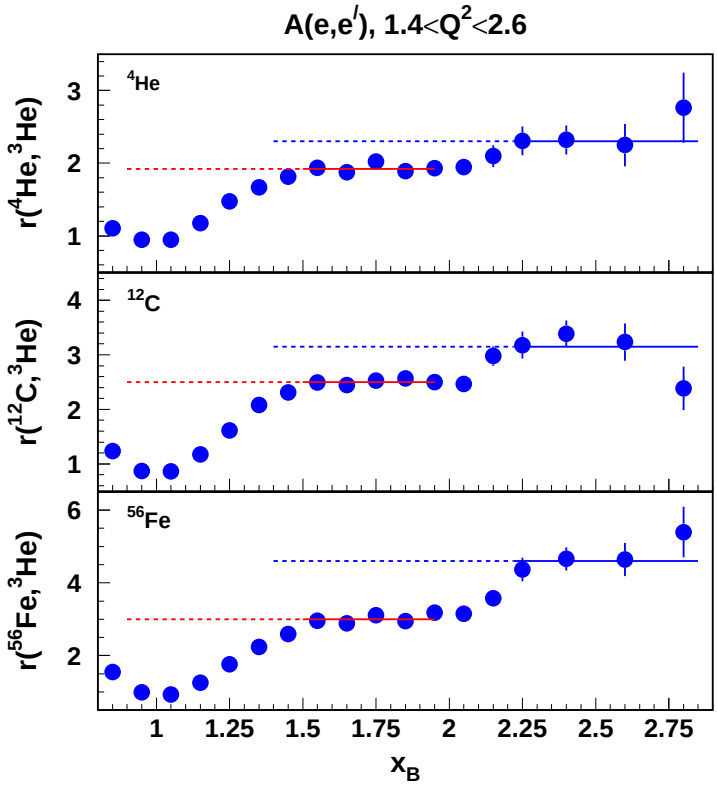

FIG. 4: Cross section (A/^{3}He) ratios at large x as measured in CLAS.

state interactions, due to the different mix of nn, np, and pp correlations in non-isoscalar nuclei. However, there are calculations indicating that there are significant final state interactions that do not vanish rapidly as Q^2 increases, and which do not cancel in the target ratios [19] (i.e. do not come from short range configurations that are identical in all nuclei). This calculation indicates that the FSI (when including inelastic channels) has a very weak Q^2 dependence and will persist, challenging our interpretation of the impulse approximation analysis. In addition, it predicts that the FSI effects will increase the $x > 1.5$ cross section in iron by approximately a factor of ten, and that even in the ratio of iron to deuterium, there is a factor of five effect from these FSIs. An important portion of the proposed measurement is the ability to test these precisions of FSIs by extracting absolute cross sections for $x > 1.5$ on a variety of few-body (and heavy) nuclei over a range of Q^2.

For the deuteron, which is dominated by the simple two-body breakup assumed in an impulse approximation analysis, we can extract the nucleon momentum distribution from the inclusive data without the complications caused by neglecting the separation energy of the full spectral function. The momentum distribution for the deuteron as extracted from experiment E89-008 is shown in Fig. 5 [3]. The normalization of the extracted momentum distribution is consistent with unity, and the high momentum components are in good agreement with calculations based on modern two-body nucleon–nucleon potentials. This sets limits on the impact of FSI, even in the region dominated by short range correlations, indicating that the scattering is consistent with the impulse approximation and that final state interactions much smaller than those observed in coincidence A(e,e'p) measurements, or those predicted in some calculations. In the proposed measurements, we will extract absolute cross sections for ^{2}H, ^{3}He, and ^{4}He, not available for the CLAS results, which will allow us to set limits on the size (and A dependence) of final state interactions.

The extension of these ratio measurements to higher Q^2 will allow us to better test the x and Q^2

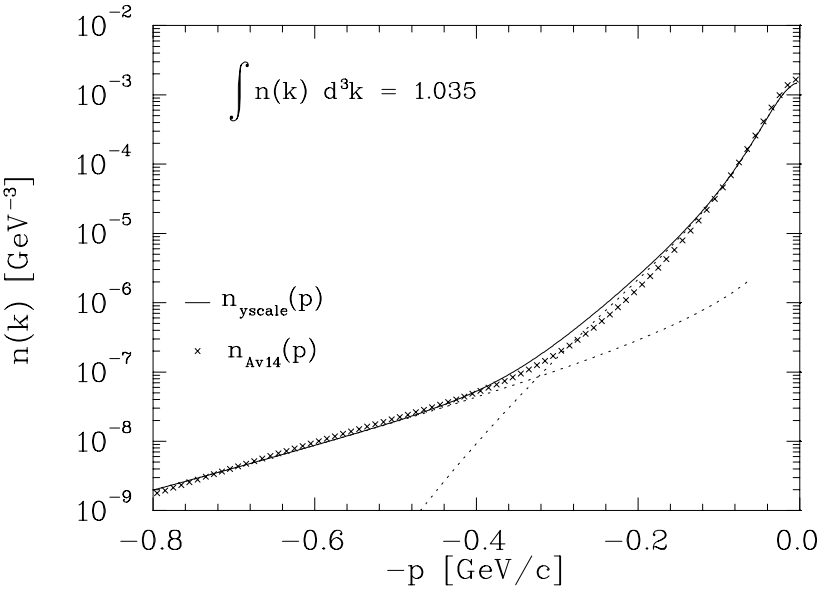

FIG. 5: The momentum distribution, n(p), for the deuteron from a fit to the E89-008 data at 4 GeV (solid line), and from a calculation using the Argonne v14 potential (crosses)

independence of the ratios in the 2N and 3N correlation regions. In addition, the extraction of the absolute cross sections for few body nuclei in this region will provide a direct constraint on final state interactions. Previous data for $x \to 2$ in deuterium already constrains the absolute size of the final state interactions, meaning that one does not have to rely on cancellation between FSI effects that could be several times larger than the impulse approximation cross section. The cross sections on ^{3}He will provide a similar test in the region of three-nucleon correlations. In addition, we will be able to use the data to directly extract the size of 2N and 3N correlations in nuclei, rather than relying on a combination of calculations of correlations in few-body nuclei, combined with ratios of A/^{2}H for 2N SRC, or A/^{3}He measurements from CLAS along with ^{3}He/^{2}H ratios from SLAC. Finally, we will be able to make comparisons of heavy nuclei to ^{4}He, to look for signatures of four-nucleon correlations, or alpha-clusters in nuclei. While we do not have measurements that can be used to predict exactly what to expect for the cross sections at $x > 3$, one expects that the larger correlations should have a smaller contribution, but also a slower falloff in x making it likely that we will be able to make precise measurements in this region.

For the 2N SRC region, data from the recent E02-019 should improve the situation, providing better absolute cross section measurements at larger x than the lower energy Hall C measurement, and covering a larger Q^2 range than the CLAS data. It will also allow us to start constraining the size of final state interactions in the few-body nuclei, but is limited in the x and Q^2 range compared to what can be accomplished with the proposed measurements at 11 GeV.

The question of the nature of the short range correlations can also be examined without relying on an impulse approximation based analysis, by directly examining the structure functions. Fig. 6 shows a calculation of the structure function per nucleon for iron, including just two nucleon correlations (solid line - from [22]), and including multinucleon correlations (dotted line - from [7]). The current data [2, 3] are consistent with the calculations including two-nucleon SRCs, and indicate that the effect of multinucleon correlations is significantly smaller than estimated in the calculation. The calculation for the two nucleon SRC contributions does not include corrections for the EMC effect, but such a calculation should be available very soon [27]. The inclusion of the EMC effect will lower the calculations somewhat, making it difficult to use this data to set a strong upper limit

on multinucleon components. The proposed measurements at 11 GeV will allow us to reach $Q^2 \approx 13(20)$ GeV^2 at $x = 1.5(1.3)$, where the calculation shows a dramatically greater sensitivity to multinucleon correlations. In addition, with data on ^{2}H, ^{3}He, and ^{4}He, it should be possible to disentangle the EMC effect from 3N correlations [27, 28]. This will allow us to either obtain a clear signal of multinucleon correlations or set significant limits on their contributions. We can also directly compare the structure function for heavy nuclei to few body nuclei in the region where the structure function is dominated by SRCs. This will provide a (model-dependent) measure of the absolute size of the contribution from correlations, as opposed to the relative contributions that can be measured in the cross section ratios. In addition, by comparing heavy nuclei to deuterium, we can look for deviations from the two nucleon SRCs, and by comparing to ^{3}He where the two nucleon correlations are small for $x > 2$, we can look for signatures of three nucleon correlations. This type of comparison is more direct than comparisons of the extracted momentum distribution from a scaling analysis.

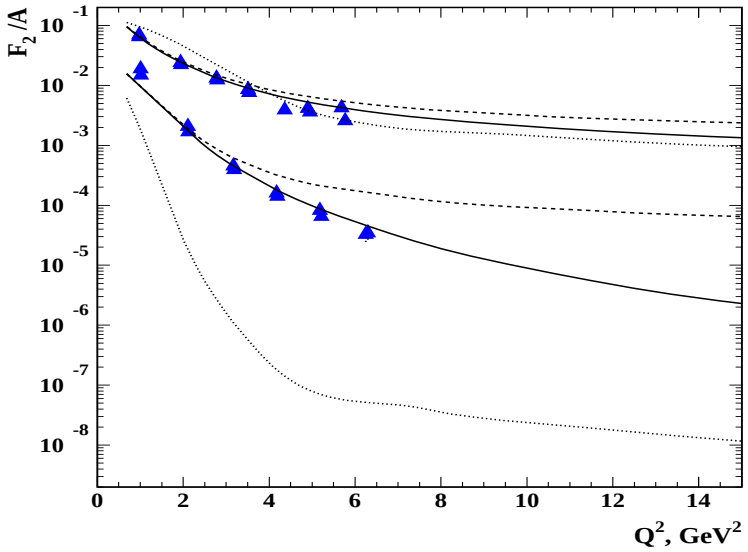

FIG. 6: Structure function per nucleon for iron from E89-008 compared to calculations without correlations (dotted lines), including two nucleon SRCs (solid lines) and multinucleon SRCs (dashed line). The upper set of data and calculations is for $x = 1$, while the lower are for $x = 1.5$. The proposed measurements will extend the data at $x = 1.5(1.3)$ to $Q^2 \approx 13(20)$ GeV^2

IV. DEEP INELASTIC SCATTERING AT $x > 1$

While previous measurements on electron-nucleus scattering at $x > 1$ have focussed on quasielastic scattering, and avoided regions where inelastic contributions have any significant contribution. The increase in energy to 11 GeV will allow us to make measurements at $x > 1$ that are dominated by deeply inelastic scattering and map out the distribution of extremely high momentum nucleons in nuclei. The response of the nucleus in the range $x > 1$ is expected to be composed of both deep-inelastic scattering from quarks in the nucleus and elastic scattering from the bound nucleons (quasielastic scattering). For both the bound quark and bound nucleon cases it is the non-zero momentum of the bound nucleons that permits scattering into a kinematic region that is forbidden

for the free nucleon. Regions dominated by scattering from the quarks should exhibit scaling in the Bjorken x variable (experimentally verified for $x < 1$), while the quasielastic scattering from the nucleons exhibits y scaling [6, 29].

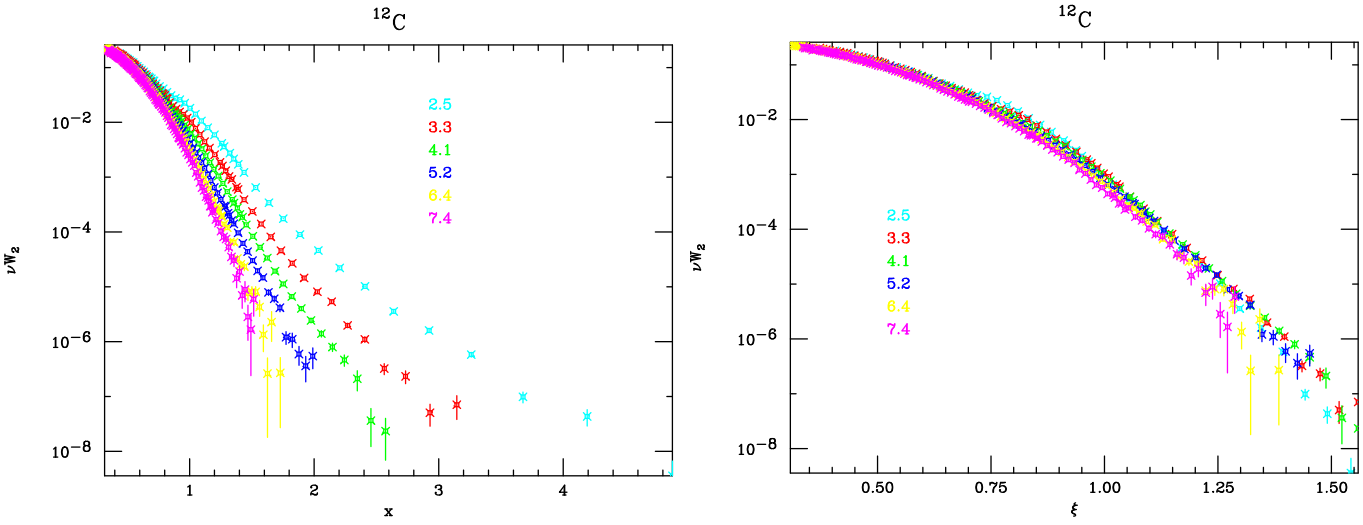

FIG. 7: Structure function per nucleon for ^{12}C vs. the Bjorken scaling variable x (left) and the Nachtmann scaling variable ξ from Jefferson Lab E02-019. The Q^2 values are given for Bjorken $x = 1$. Data are preliminary and errors shown are statistical only.

Deviations from scaling in DIS come from the running of the strong coupling constant, target mass corrections, and higher twist contributions. Target mass corrections are important at lower Q^2 values, especially at large x values, as their contribution is roughly proportional to x^2/Q^2. This can be seen clearly from the previous SLAC and JLab results [4, 30], as well as the recent E02-019 data. A common prescription for treating target mass corrections is to study the Q^2 dependence of F_2 as a function of the Nachtmann variable ξ,

$$\xi = 2x/(1 + \sqrt{1 + 4M^2x^2/Q^2}) \tag{1}$$

rather than Bjorken x (note that $\xi \to x$ for $Q^2 \to \infty$). Figure 7 shows F_2 for carbon as a function of x and ξ for a variety of Q^2 values from E02-019. When taken as a function of x, there are clear scaling violations at large x, even for $x < 1$. When taken vs ξ, the scaling violations at smaller ξ values are consistent with the QCD evolution of the structure function. However, the remaining quasi-elastic contribution in the Q^2 range of this data is still large enough to provide introduce clear scaling violations at the larger ξ values; the quasielastic peak is visible at $\xi \approx 0.8$ for the smallest Q^2 values, but decreases in size and moves towards $\xi = 1$ as Q^2 increases. This can be seen more clearly in deuterium (see Figure 8) where the quasielastic peak is more clearly visible due to the smaller Fermi motion. Note that even for deuterium, the Delta contribution does not yield appreciable scaling violations, even for the lowest Q^2 values shown, while the scaling violations on the top of the quasielastic peak decrease dramatically over the Q^2 range of the measurement.

The structure function measured in E02-019 shows scaling in the Nachtmann variable ξ, even at large values of ξ, where the scattering has very large resonance or even quasielastic scattering contributions. This can be understood in terms of local duality, which leads to scaling *on average* of the proton structure function, and which leads directly to scaling for the nuclear structure function (the necessary averaging coming from the Fermi motion of the nucleons). This can also be viewed in

terms of a near complete cancellation of the large higher twist contributions in the resonance region. In retrospect, it is not surprising that the nuclear structure function shows ξ-scaling in the resonance region, given the quantitative success of local duality in the proton structure function. This duality is seen if one averages over the entire resonance region or even if one averages in the region of a single resonance. In the nucleus, the Fermi motion of the nucleons performs this averaging and duality yields true scaling, rather than scaling on average, in regions where the intrinsic averaging is sufficient.

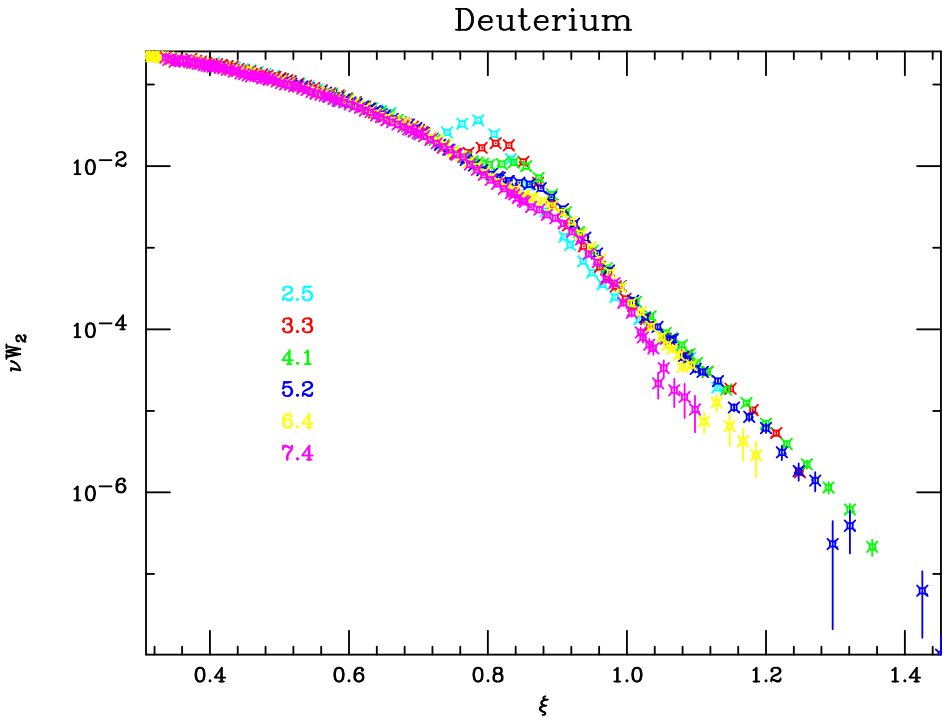

FIG. 8: Structure function per nucleon for deuterium vs. the Nachtmann scaling variable from Jefferson Lab E02-019. The Q^2 values are given for Bjorken $x = 1$. Data are preliminary and errors shown are statistical only.

At 11 GeV, we can reach Q^2 values large enough that even the cross section at $x \simeq 1$ is dominated by DIS scattering (scattering with $W^2 > 4$ in the electron-nucleon system). Figure 9 shows the breakdown of the cross section for scattering at 22° and 55°, based on the convolution model described in [31]. At 22°, the data is dominated by DIS scattering only for $x \lesssim 0.7$, and is dominated by quasielastic and resonance contributions at large x values. This corresponds to our lowest scattering angle for the high-Q^2 studies, but the section is at significantly larger Q^2 than any of the 6 GeV data from E02-019. Nonetheless, the data from E02-019 shows precise scaling of the structure function up to $\xi \approx 0.8$, with relatively small scaling violations even in the region dominated by the quasielastic peak (see Fig. 8). While the cross section at 22° is dominated by quasielastic and resonance contributions, with the DIS contributing <20% for $x \gtrsim 1.2$, the situation is different at larger Q^2 values. For scattering at 55°, the quasielastic contributes $\lesssim$10% over the full x range shown, while the resonance and DIS provides $\gtrsim$80% of the cross section up to x=1.3. Given the quality of the scaling observed in E02-019, it seems likely that the resonance contributions to the cross section at the much larger Q^2 values of this proposal will yield extremely small deviations from the scaling limit structure functions. We will be able to verify this over a good part of the x range by combining the Q^2 dependence from this and previous measurements.

While there will always be some contribution from lower lying resonances and quasielastic scattering, this contribution becomes small at the large Q^2 values accessible in this measurement. In

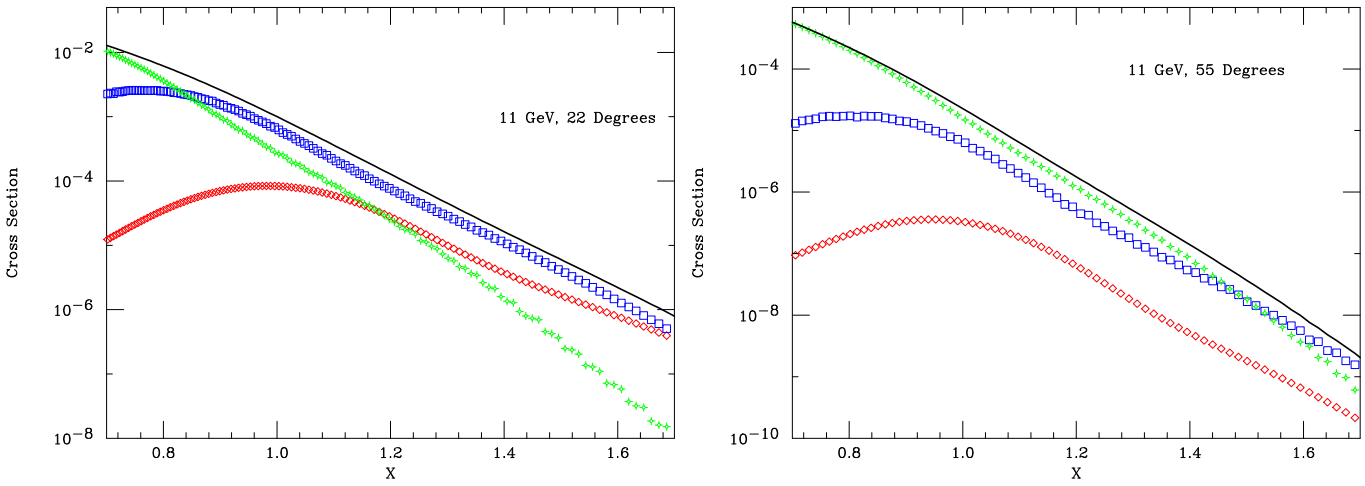

FIG. 9: Breakdown of the contributions to the inclusive cross section as a function of x for scattering at 11 GeV and 22° (left) and 55° (right) with and 11 GeV beam calculated in a convolution model[31]. The red diamonds indicate quasielastic contribution, the blue boxes show the contribution from the resonance region ($W^2 < 4$ GeV^2), and the green stars indicate the contribution from DIS scattering ($W^2 > 4$ GeV^2 in the photon-nucleon system).

addition, the E02-019 data, taken at much lower Q^2 values ($Q^2 \lesssim 7$ GeV^2 for $x = 1$), shows approximate scaling even in the regions dominated by scattering at $W^2 < 4$ GeV^2. So not only is the size of the contribution from lower W^2 scattering quite small, it appears to be consistent with the DIS contribution, yielding very small scaling violations at lower Q^2, and presumably extremely small scaling violations at the Q^2 where it provides a very small contribution to the cross section. We will take data to map out the Q^2 dependence, as a check that the scaling violations continue to decrease as one goes to higher and higher Q^2 values.

A. Distribution of superfast quarks

This extended scaling for nuclei also means that the nuclear structure function as measured in the DIS region is the same as the structure measured at lower values of W^2. This scaling may allow measurements of the quark distributions in nuclei at lower Q^2 (or equivalently lower Q^2 for fixed ξ) than accessible if one requires $W^2 > 4$ GeV^2. This will allow us to examine the ξ-dependence of the structure function for large values of ξ. The structure functions have been measured at extremely high Q^2 values (~ 100 GeV^2) in μ−C scattering [32] and ν-Fe scattering [33]. Near $\xi = 1$, these experiments obtained significantly different results. The neutrino experiment (CCFR) found $F_2^{Fe} \propto \exp(-8.3x)$ (at these Q^2, the difference between ξ and x is relatively small), consistent with a significant contribution from superfast quarks in the nucleus. The CCFR data is shown Figure 10.

The muon experiment (BCDMS) found a much different behavior for the structure function with $F_2^C \propto \exp(-16.5x)$ (Figure 11), which is a dramatically faster falloff than obtained from the CCFR data. The BCDMS data has much lower statistics, while the CCFR experiment has a much poorer resolution in x, and both experiments have limited x coverage, making it difficult to directly compare the results (especially since the CCFR measurement does not extract the structure function, but instead compares the measured yield to the yield as calculated in their simulation for a given input structure function). While the measurements were taken on different nuclei, one would expect the carbon and iron structure functions to be very similar, and a *larger* contribution from superfast quarks for iron, due to the small increase in Fermi momentum.

This dependence was measured for C, Fe, and Au targets by E89-008, and for all targets the

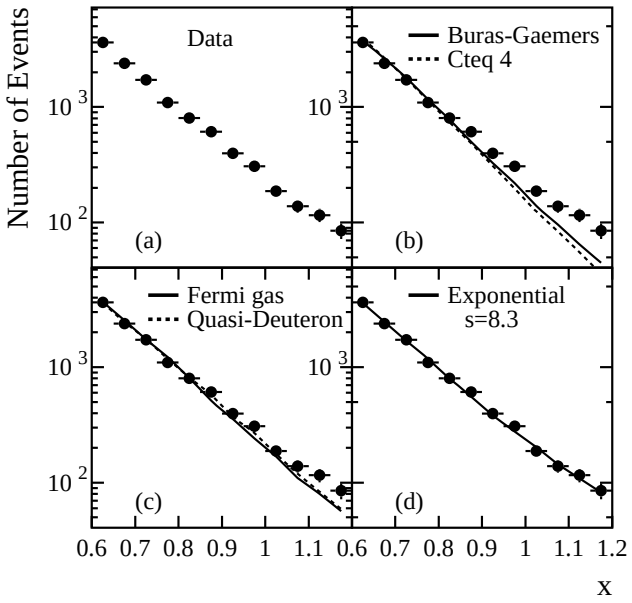

FIG. 10: CCFR distribution of events as a function of x, compared to some PDF fits (top right and lower left), and compared to a fit of $F_2^A \propto \exp(-sx)$, for s=8.3 (lower right).

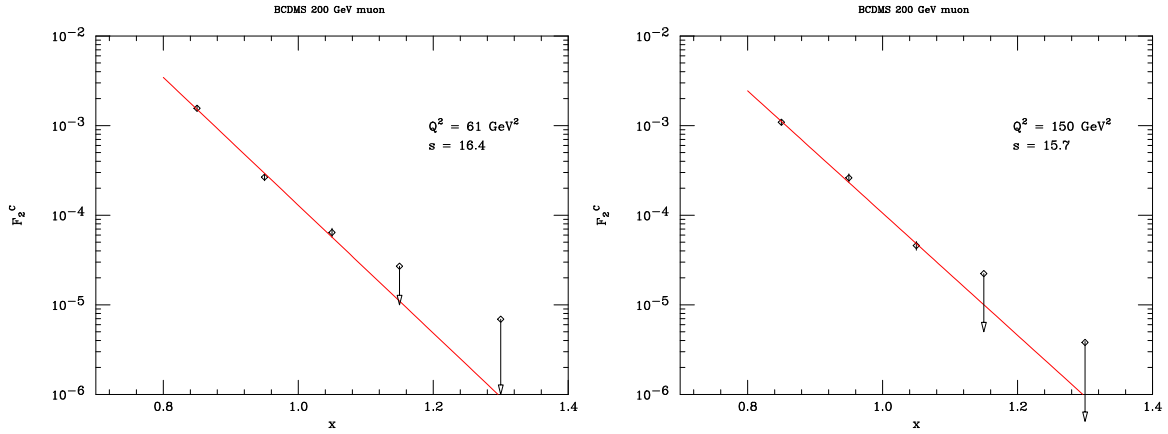

FIG. 11: BCDMS 200 GeV muon data from C. An exponential fit of $F_2^A \propto \exp(-sx)$) agrees with the JLAB 89-008 data with an exponent $s \simeq 16$ when fit in ξ

dependence was in general agreement with the BCDMS measurement with $F_2^A \propto \exp(-s\xi)$ with $s \simeq 16$. However, there are significant contributions from the quasielastic peak in the vicinity of $\xi = 1$ at these kinematics, and there is still some Q^2 variation to the structure function fall off at the largest Q^2 values from E89-008. With the proposed measurements, we can reach Q^2 values of 20 GeV^2 for $\xi \geq 1$, where quasielastic scattering is only a small contribution to the total cross section and scaling violations should be much smaller than those observed in previous measurements.

B. Sensitivity to Quark Degrees of Freedom in Nuclei

The EMC effect provides clear evidence that the quark distribution in nuclei is not a simple sum of the quark distributions of it's constituent protons and neutrons. Many explanations of the EMC effect were proposed which involved non-hadronic degrees of freedom in the nucleus. Many were ruled

out as source of the EMC effect, because they would require very large non-hadronic components which were often excluded by other measurements. Figure 12 provides a simple example: It shows the nuclear structure function for deuterium, as calculated from a convolution of neutron and proton structure functions (red), and compares it to the structure function obtained by assuming that 5% of the deuteron wave function is described by a 6-quark bag, using the model of Mulders and Thomas [34] for the quark distribution for the 6-q bag. The difference is at most 2% throughout the region of large EMC effect ($0.3 < x < 0.8$), and so one would need an extremely large exotic component in nuclei to explain the EMC effect in terms of this kind of non-hadronic contribution in nuclei.

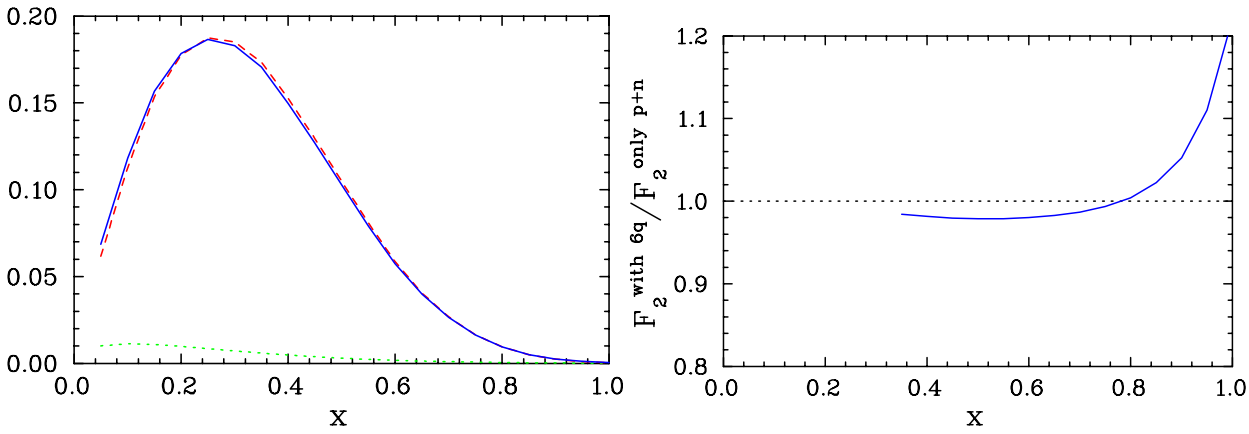

FIG. 12: The left figure shows the Deuteron valence quark distribution from a convolution of proton and neutron quark distributions (dashed red), and with the inclusions of a 5% 6-quark bag component (blue). The dotted green line shows the contribution from the 6-quark bag component. The right figure shows the ratio of F_2 with the 6-quark bag contribution to F_2 with no 6-quark contribution.

Many of these early models attempted to explain the entire EMC effect in terms of exotic explanations, while we now know that much (if not all) of the effect at large x is due to binding. While there is insufficient data at present to make precise comparisons between calculations of binding effects and the data, it is clear that non-hadronic degrees of freedom do not need to be large enough to explain the 10-20% modifications to the quark distributions in nuclei.

One can gain orders of magnitude more sensitivity to such configurations by examining the structure function at $x > 1$. A six-quark bag contribution breaks down the individual identities of the two nucleons, allowing a greater sharing of momentum between the quarks in the two nucleons and enhancing the distribution of high-momentum quarks. While this has a small impact in the region of the EMC effect, it has a much larger effect at $x > 1$, where the quark distributions fall off extremely rapidly. Figure 13 shows the same models of the quark distributions in deuterium as Fig. 12: A convolution of proton and neutron quark distributions, and a mix of 95% proton plus neutron, and 5% contribution from a 6-quark bag. In this case, the quark distribution for the simple convolution model dies off rapidly above $x = 1$, and so the contribution from the 6-quark bag can lead to enhancements of 100's of percent in the structure function, compared to the percent level effects observed for $x < 1$. While we show here the example of a 6-quark bag, any configuration in which there is direct sharing of the momentum between the quarks in the two nucleons will lead to an enhancement of this kind, with a similar increase in sensitivity in these large x structure functions. Larger effects might be observed in heavier nuclei, but one needs a quantitative understanding of the distribution of high momentum nucleons to provide a reliable "baseline" calculation for the purely hadronic picture. Measurements of quasielastic scattering at large missing momentum, planned for 6 and 12 GeV, combined with the large x ratios proposed here, should provide significant information

on the short range correlations that provide the high-momentum part of the spectral function, and allow us to separate the contribution of superfast quarks that come from high-momentum nucleons and those that come from other configurations in nuclei.

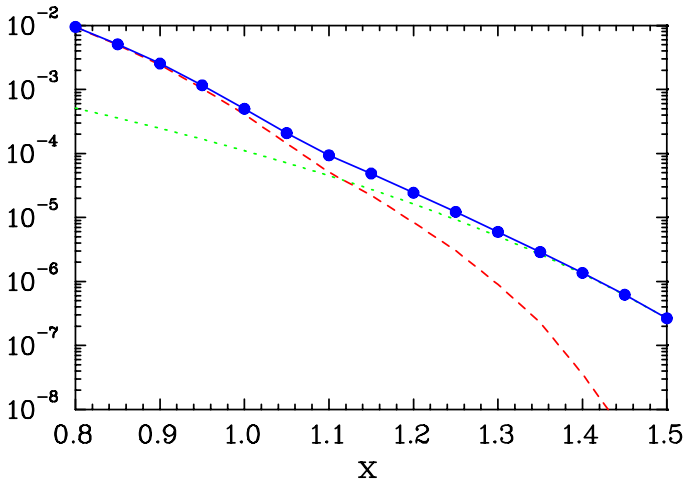

FIG. 13: Same as Fig. 12, but showing the effect of a small 6-quark bag component in the large x region. The blue circles indicated the projected measurements, with uncertainties smaller than the points shown.

Here we will be DIS dominated at least up to $x = 1.3$; however, for higher x values, the quality of scaling at lower Q^2 indicates that deviations from the scaling limit should be relatively small even for $x = 1.4 - 1.5$. Our measurements of the Q^2-dependence for selected targets will allow us to investigate this.

We can see from Fig. 6 that for large x and Q^2, the scattering is dominated by scattering from the short range correlations in nuclei. This makes it clear that it will still be important to have quantitative measurements of the contributions of short range correlations, although any uncertainty in our knowledge of the strength and detailed structure of these contributions will partially cancel in the ratio. It also provides another way to view the sensitivity to these non-hadronic components. The cross section is dominated by scattering from these short range correlations, which represent two or more nucleons in very close proximity, and therefore represents scattering from a high density configuration in the nucleus. It is then natural that one would have much greater sensitivity to modification of the nucleon structure when using the scattering kinematics to isolate scattering from high density configurations, thus probing the quark structure as a function of local density, rather than average nuclear density.

V. OTHER TOPICS OF INTEREST

In addition to providing information about short range correlations and parton distributions at $x > 1$, these measurements will provide data that can be used to study duality and to make precise measurements of the nuclear dependence of QCD moments. Current moment analyses are limited at moderate to high Q^2 values by the knowledge of the structure function at $x > 1$, especially for the higher moments [35]. Combining this data with lower x measurements from duality studies of hydrogen and deuterium will allow a more precise determination of the first several moments of the nuclear structure function. A comparison of the moments of deuterium and hydrogen may allow a determination of the moments for the neutron without some of the theoretical ambiguities that arise when attempting to directly extract the neutron structure function from data on nuclei.

This data will also provide new ways to probe the details of duality in nuclei [4, 30, 36, 37]. Studies

of duality in the proton have shown that the resonance region structure function is consistent with the scaling limit, when averaged over an the resonances [36, 38, 39]. This duality has been observed for both the global average over the resonance region and for the local average in the vicinity of the prominent resonances. However, the duality breaks down if one takes only a very narrow region, for example, if one take a narrow region on top of a prominent resonance, then the structure function will be larger than the scaling limit structure function. In nuclei, Fermi motion provides an averaging of the structure function, thus providing an explanation of the observed ξ scaling as a direct consequence of duality in the proton and neutron. However, at larger ξ values, in particular for $\xi > 1$, it is not clear that this connection should hold [31]. At low Q^2, scattering at $\xi > 1$ is dominated by the low-energy transfer side of the quasielastic peak, and so it is not clear that the averaging provided by Fermi motion will sample a large enough region to yield scaling, as duality does not hold if one looks at too narrow a region of W^2, for example, looking only in region of the tail of a resonance (or in this case, the quasielastic peak). At larger Q^2, however, the cross section has significant quasielastic, resonance, and DIS contributions, as seen in Fig. 9, and so it may well be that at sufficient Q^2, duality in the nucleon structure function may be sufficient to explain scaling of the nuclear structure function even for $x > 1$. This data will allow for a careful examination of both the ξ and Q^2 dependence, and map out the onset of scaling.

VI. DETAILS OF THE 11 GEV PROPOSED MEASUREMENTS

A. Backgrounds and Systematic Errors

While probing different physics than previous measurements, this experiment is, from a technical point of view, a relatively straightforward extension of the lower energy measurements of inclusive scattering from nuclei. The dominant sources of background are the pion contamination of the electron distribution and charge symmetric background. In the previous runs, this contamination was always less than 1% in the HMS when using the calorimeter and Čerenkov information for particle identification. While the pion background will be somewhat worse at these larger energies, the main limitation at lower energies was the pion rejection in the calorimeter when the scattered electron was at low momentum. In this proposal, the minimum scattered electron energy is significantly higher; 1.5 GeV for the HMS, and 4 GeV for the SHMS, and the pion rejection should be sufficient for the proposed kinematics.

Of greater concern was the background from secondary electrons produced in the target. The main source likely comes from electro-production and photo-production of neutral pions. These pions then decay into photons which can produce position-electron pairs. This background is charge-symmetric, and can be measured directly by changing the spectrometer to positive polarity and detecting the produced positrons. For the largest angles measured in E89-008 (55° and 74°), this background was significant and required a fit to our positron measurements and subtraction from our electron data (see Ref. [24] for more details). The data from E02-109, taken at 5.8 GeV, show charge symmetric backgrounds of ∼10% for the largest angle, decreasing rapidly as the scattering angle is decreased. This background is sensitive to the radiation length and geometry of the target, and will have to be measured and subtracted for the large scattering angle data. As a result, we will limit our running 55°, and have included time in our beamtime request to measure this background.

The combined systematic uncertainties from the E89-008 run totaled 3.2 to 4.7% for the HMS data with the primary contributors being knowledge of the acceptance, radiative corrections, target thickness,and bin centering (correcting an integral number of counts within a momentum/angle bin to the measured cross section at the center of the bin). Each of these four items ranged from approximately 1% to 2%, depending on the scattering angle. Table 1 summarizes the systematic

TABLE I: Systematic uncertainties in the extraction of the cross section for 4 GeV running. Entries with an asterisk indicate that a correction was made directly to the cross section which had the listed uncertainty. Entries without an asterisk indicate no correction to the cross section, just a contribution to the overall uncertainty.

Systematic	HMS
Acceptance Correction	1.0-2.2%*
Radiative Correction	2.5%*
Target Track Cuts	0.5%
Bin Centering Correction	1.0-2.2%*
PID Efficiency	0.5%*
Charge Measurement	1.0%
Target Thickness	0.5-2.0%
Target/Beam Position Offset	0.25%
Tracking Efficiency	0.5%*
Trigger Efficiency	0.05%*
Normalization	0.0%
COMBINED UNCERTAINTY	3.2-4.7%

uncertainties during the 4 GeV running. Preliminary results on the E02-019 indicate that we should achieve similar uncertainties.

There is an additional uncertainty in the extraction of F_2 from the cross section due to the uncertainty in $R = \sigma_L/\sigma_T$. This was generally negligible, except at the largest x and Q^2 values measured.We will take a small amount of data with ~ 4 GeV beam, both as a cross calibration with the previous measurement and also to provide a rough determination of R. In the E89-008 analysis, a value of $R = 0.32/Q^2$ was assumed, with a 100% uncertainty in this value. For the proposed 11 GeV measurements, these uncertainties are smaller than in the previous measurements, and contribute at most 1-1.5% to the uncertainty.

B. Proposed Kinematics with 11 GeV Beam

Fig. 14 shows the kinematic range in x and Q^2. The region below the dashed (solid) curve is what is accessible with 4 (6) GeV beam at JLab ($\theta \leq 60^\circ$ in both cases). Experiments E89-008 and E01-019 did not cover the full Q^2 range for very large x values, so the existing data for $x > 2.2$ is limited to $Q^2 \lesssim 5$ GeV^2. Previous SLAC measurements of inclusive electron scattering from nuclei [2] were limited to $x \leq 3$ and $Q^2 \leq 3$ GeV^2. As with E02-019 we have included ^{3}He and^{4}He cryogenic targets.

The increase in beam energy to 11 GeV will have the greatest impact on the Q^2 range for kinematic points with $1.0 \lesssim x \lesssim 1.5$. This extended Q^2 data is critical to studies of the extremely large x quark distributions. At larger values of x, the Q^2 increase is smaller but is crucial for studies of the nature of the short range correlations. The increase in Q^2 is enough to allow us to reach well into the scaling region ($Q^2 \gtrsim 3$ GeV^2) out to extremely large x values. This will allow us to verify that the cross section ratios for $x > 2.25$ are independent of Q^2, and provide direct extractions of the relative strength of 3N correlations in a variety of nuclei. In addition, the measurements of the absolute cross sections at large x from few-body nuclei up to A=4 will provide tests of final state interactions, which would interfere with the interpretation of these ratios in terms of multi-nucleon correlations. The existing data from the E02-019 measurement at 6 GeV will provide high quality measurements of the ratios and absolute cross sections in the region up to $x = 2$, and provide a first look at the Q^2 dependence and absolute cross sections for the region up to $x = 3$. The proposed

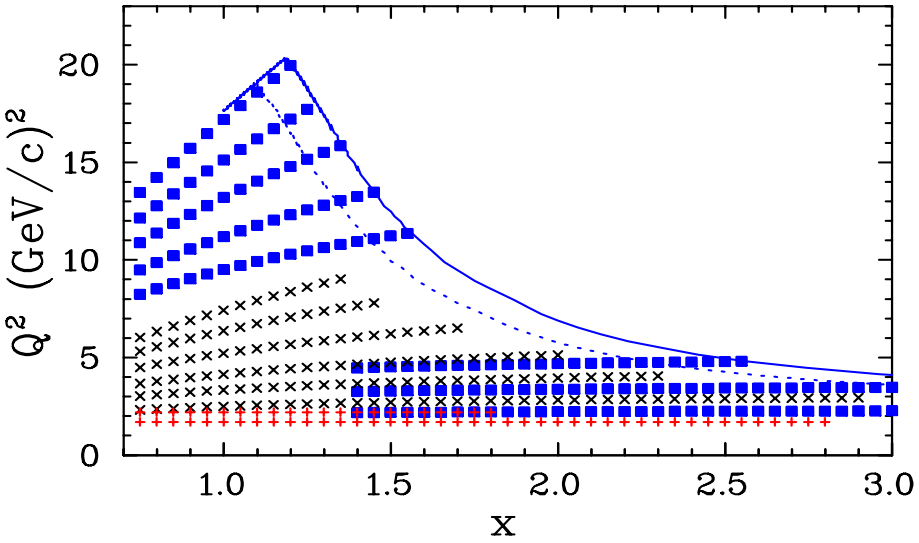

FIG. 14: The kinematic range in Q^2 and the Bjorken x variable. The black symbols indicated the range with a 6 GeV from E02-019, the red reflect that obtained in the CLAS ratio measurements. The blue symbols and line define the region accessible at 11 GeV. The solid (dashed) blue curve indicates the region where the projected statistical uncertainties are 10% (5%) for an x bin of 0.05.

measurements at 11 GeV will be able to make significantly improved measurements up to $x = 3$, and provide a first look at larger x, where one might observe the dominance of scattering from alpha-clusters (four-nucleon correlations) in nuclei.

C. Experimental Equipment

The experimental set-up for measurements with a 11 GeV beam would be performed using the existing HMS and new SHMS which is part of the base equipment package for the 12 GeV upgrade. The HMS would be used for the highest Q^2 measurements at large angles and the SHMS would be used for the intermediate angles, $\lesssim 30^\circ$ providing the intermediate Q^2 measurements for $x \lesssim 1.5$, and the modest Q^2 but very large x measurements. Data would be taken in the HMS spectrometer using the existing detector package which includes a threshold gas Čerenkov counter and a lead glass shower counter for rejection of pion background. The SHMS will have a similar package of nearly identical performance. Several nuclear targets (Be, C, Cu, and Au) would be used as well as cryogenic targets. We will run at beam currents between 20 and 80 μA.

A cryogenic hydrogen target is necessary for calibration and a cryogenic deuterium target for production data. These are currently part of the standard Hall C cryotarget system. ^{3}He and ^{4}He cells have been used in E02-019, and we found that these cells performed extremely well at currents up to 80μA. In addition to the cryotargets, we will take data on several solid targets, Be, C, Cu, and Au, which will allow us to measure the A dependence of the contributions from short range correlations, the A dependence of the quark distributions at $x > 1$, as well as allowing for an extrapolation to nuclear matter. The measurements would be done at several angles to cover the full kinematic range, as shown in Fig. 14 and listed in Table II.

We assume an acceptance of 6.8msr for the HMS, and 3.8msr for the SHMS, and will take data independently with both spectrometers throughout the run. The SHMS will make all of the measurements for the very large x, where we are focussed on the short range correlations. For the data focussed on extracting the distribution of superfast quarks, the HMS will take the largest Q^2 mea-

θ (deg)	E' settings (GeV)	x	Q^2 GeV^2	time(hrs) Cu	Notes
8.0	10.6	0.7-4.0	2.1-2.3	10	SHMS (17 hrs. for cryotargets)
10.0	10.4	0.7-3.0	3.0-3.5	10	SHMS (17 hrs. for cryotargets)
12.0	9.8	0.7-2.6	4.0-5.0	10	SHMS (17 hrs. for cryotargets)
22.0	5.7,7.0	0.7-1.55	8.1-12	3+8=11	SHMS
26.0	4.8,6.0	0.7-1.45	9.5-14	3+8=11	SHMS (use HMS for cryotargets)
32.0	3.3,3.9,4.6	0.7-1.35	11-17	(1+5+10)	HMS
40.0	2.4,2.8,3.3	0.7-1.25	12-18	(1+5+10)	HMS
55.0	1.5,1.7,2.0	0.7-1.20	13-20	(2+8+10)	HMS
				12	e^+ data
				6	overhead
				6	dummy targets (cryotargets only)
				70 (87)	Total time for Cu (LD2)

TABLE II: Kinematics and runtimes for the Cu running. Data taking with the HMS is simultaneous with SHMS running, and so the times in parenthesis are not included in the total. For the cryogenic targets, data taking at 26 degrees, will be taken with the HMS to allow extra SHMS running time for the very large x data on the cryotargets. In addition, extra time is required for measurements on a "dummy" target, used to measure the contribution from the target endcaps.

surements, which require scattering angles beyond 30 degrees, and the SHMS will take some of the lower Q^2 measurements. We will also take data for deuterium and carbon with both spectrometers at the same kinematics, to perform a cross check on the extracted cross sections.

VII. REQUEST TO LABORATORY

The kinematics and runtimes for the Cu data taking are listed in Table II, assuming 80μA running on a 6% radiation length target. The total runtime for Cu is 70 hours, including over head and positive polarity measurements of the charge-symmetric background. Including Be, C, and Au (scaling run times by the target nucleon densities) yields a total runtime of 259 hours for the solid targets.

The deuterium target has roughly the same nucleon arial density as the copper target, so the runtime for deuterium is essentially the same as given in Table II. However, for the cryogenic targets, more time is required at the smaller angles which cover the extremely large x values, as the subtraction of the aluminum endcap contributions are important, and the cross section in the correlation dominated regions are a few times smaller than for the solid targets. For these kinematics, we will take the data at 26° with the HMS (using three momentum settings), bringing the HMS runtime (neglecting positron running and overhead) from 52 to 63 hours, and allowing us to roughly double the running time for the small angle data on the cryotargets. This brings the runtime for deuterium up from the 70 hours given in table II to 81 hours, plus an additional six hours of running on the dummy target, for 87 total hours on deuterium. While the deuterium data is only measured up to $x = 2$, the entire large-x region is covered in a single setting of the SHMS, so the kinematics are the same for ^{3}He and ^{4}He. Scaling the runtime by effective thickness of the ^{3}He and ^{4}He, we require a total running time of 383 hours.

The total beam time request is summarized in Table III. This includes time for cross-calibrations of the HMS and SHMS at 26 degrees for deuterium and carbon, target heating studies, BCM calibrations and beam spot size monitoring, hydrogen elastics studies, and checkout and commissioning time. Because the Helium targets and hydrogen/deuterium targets can not run at the same time, we also include time for a changeover between the hydrogen and helium targets. The sum time for

Activity	Time (hours)
Solid target running	259
Cryotarget running	383
HMS/SHS cross calibration	16
Hydrogen elastics	24
Target Boiling Studies	16
Target Changeover	24
BCM calibrations	8
Beam spot monitoring	4
checkout/calibration	24
Total	758 (32 days)

TABLE III: Beam time request for the proposed experiment. The time shown is for SHMS running; HMS running is parasitic.

checkout, calibration and beam studies is 116 hours, making the total beamtime request 758 hours, or 32 days.

VIII. SUMMARY

We propose to measure inclusive scattering at $x > 1$ on several light and heavy nuclei. The data is broken into two kinematic regions. Data taken at moderate Q^2 values for extremely large x, where the cross section ratios are sensitive to the presence of two-nucleon and multi-nucleon correlations. The cross section ratios at very large x will allow us to study in detail the A dependence of the strength of 2N and 3N SRCs. The larger Q^2 values of the proposed measurements, along with the ability to make absolute cross section measurements will allow us to verify the assumptions made in previous studies. The coverage should also allow for first studies of the size and importance of α-clusters in nuclei.

This data will complement the many completed and upcoming coincidence$A(e, e'p)$ and $A(e, e'NN)$ measurements attempting to probe the high momentum components of the spectral function and short range correlations [40–42]. The inclusive measurement can reach much larger values of the missing momentum, where the coincidence measurements become cross section (or background) limited. The inclusive measurements are also cleaner,being significantly less sensitive to final state interactions, meson exchange currents, and other processes which must be modeled in the analysis of the coincidence measurements. In the inclusive measurement, one does not reconstruct the excitation energy of the final system (the missing energy of the struck nucleon), and so is sensitive to the entire missing energy distribution of the spectral function. Both inclusive and coincidence experiments are important in these studies, as inclusive measurements can provide fairly clean information on the very high momentum components of the spectral function, while the coincidence experiments can provide detailed information on the missing energy distribution (and momentum distributions for the individual shells) at lower momentum values.

The second physics goal is the extraction of the structure functions, and thus the unseparated quark distributions, at $x > 1$. The existing measurements from neutrino and muon scattering are of limited statistical precision and kinematic coverage, and yield contradictory results. Nuclear dependence of the structure functions at $x > 1$ can provide new insight into the origin of the EMC effect [43], and the distribution of these superfast quarks in nuclei is extremely sensitive to

non-hadronic components, providing orders of magnitude more sensitivity to configurations such as 6-quark bags.

In addition to the main goals of studying short range correlations and parton distributions at $x > 1$, this data will also allow several other studies. It will allow us to extended measurements of duality and scaling in nuclei, especially for $\xi > 1$ where it is not clear whether or not ξ-scaling is a natural consequence of local duality [31]. In addition, measurements of the structure function in nuclei at large values of x are important in the extraction of QCD moment in nuclei, especially for the higher moments which are extremely sensitive to the contributions at large x.

[1] D. B. Day et al., Phys. Rev. Lett. **43**, 1143 (1979).
[2] D. B. Day et al., Phys. Rev. Lett. **59**, 427 (1987).
[3] J. Arrington et al., Phys. Rev. Lett. **82**, 2056 (1999).
[4] J. Arrington et al., Phys. Rev. C **64**, 014602 (2001).
[5] J. Arrington, D. Day, B. Filippone, A. F. Lung, et al., Jefferson lab experiment E02-019.
[6] D. B. Day, J. S. McCarthy, T. W. Donnelly, and I. Sick, Ann. Rev. Nucl. Part. Sci. **40**, 357 (1990).
[7] L. L. Frankfurt and M. I. Strikman, Nucl. Phys. **B181**, 22 (1981).
[8] C. C. degli Atti and S. Simula, Phys. Lett. B **325**, 276 (1994).
[9] O. Benhar and S. Liuti, Phys. Lett. B **358**, 173 (1995).
[10] B. L. Ioffe, V. A. Khoze, and L. N. Lipatov (1984), amsterdam, Netherlands: North-holland 340p.
[11] E. Pace, G. Salmè, and G.B.West, Phys. Lett. B **273**, 205 (1991).
[12] O. Benhar et al., Phys. Rev. C **44**, 2328 (1991).
[13] O. W. Greenberg, Phys. Rev. D **47**, 331 (1993).
[14] B. L. Ioffe, JETP Lett. **58**, 876 (1993).
[15] E. Pace, G. Salme, and A. S. Rinat, Nucl. Phys. **A572**, 1 (1994).
[16] S. A. Gurvitz and A. S. Rinat, Phys. Rev. **C47**, 2901 (1993).
[17] A. S. Rinat and M. F. Taragin, Nucl. Phys. **A620**, 417 (1997).
[18] A. S. Rinat and M. F. Taragin, Nucl. Phys. **A624**, 773 (1997).
[19] O. Benhar, Phys. Rev. Lett. **83**, 3130 (1999).
[20] L. L. Frankfurt and M. I. Strikman, Phys. Rept. **160**, 235 (1988).
[21] L. L. Frankfurt, M. M. Sargsian, and M. I. Strikman, Phys. Rev. **C56**, 1124 (1997), nucl-th/9603018.
[22] L. L. Frankfurt, M. I. Strikman, D. B. Day, and M. Sargsian, Phys. Rev. **C48**, 2451 (1993).
[23] K. S. Egiyan et al. (CLAS), Phys. Rev. **C68**, 014313 (2003).
[24] J. Arrington, Ph.D. thesis, California Institute of Technology (1998).
[25] K. S. Egiyan et al. (CLAS), Phys. Rev. Lett. **96**, 082501 (2006).
[26] K. Egiyan et al., cLAS-NOTE 2005-004, www1.jlab.org/ul/Physics/Hall-B/clas.
[27] M. M. Sargsian, private communication.
[28] M. I. Strikman, private communication.
[29] O. Benhar, D. Day, and I. Sick (2006), nucl-ex/0603029.
[30] B. W. Filippone et al., Phys. Rev. C **45**, 1582 (1992).
[31] D. Day and I. Sick, Phys. Rev. **C69**, 028501 (2004).
[32] A. C. Benvenuti et al. (BCDMS), Phys. Lett. B **189**, 483 (1987).
[33] M. Vakili et al. (CCFR), Phys. Rev. **D61**, 052003 (2000), hep-ex/9905052.
[34] P. J. Mulders and A. W. Thomas, Phys. Rev. Lett. **52**, 1199 (1984).
[35] I. Niculescu, J. Arrington, R. Ent, and C. E. Keppel, Phys. Rev. **C73**, 045206 (2006), hep-ph/0509241.
[36] W. Melnitchouk, R. Ent, and C. Keppel, Phys. Rept. **406**, 127 (2005).
[37] J. Arrington, R. Ent, C. E. Keppel, J. Mammei, and I. Niculescu, Phys. Rev. **C73**, 035205 (2006).
[38] I. Niculescu et al., Phys. Rev. Lett. **85**, 1182 (2000).
[39] Y. Liang et al. (2004), nucl-ex/0410027.
[40] D. Rohe et al., Phys. Rev. Lett. **93**, 182501 (2004).
[41] M. M. Rvachev et al. (The Jefferson Lab Hall A), Phys. Rev. Lett. **94**, 192302 (2005).
[42] W. Bertozzi, E. Piasetzky, J. Watson, S. Wood, et al., Jefferson lab experiment E01-015.
[43] D. F. Geesaman, K. Saito, and A. W. Thomas, Ann. Rev. Nucl. Sci. **45**, 337 (1995).